RSBO

ISSN:
Electronic version: 1984-5685
RSBO. 2013 Oct-Dec;10(4):318-25

Original Research Article

Colorimetric photoelastic analysis of tension distribution around dental implants

João César Zielak[1]
Marcelo Filietaz[1]
Felipe Belmonte Archetti[2]
Paulo Roberto Camati[1]
Thalyta Verbicaro[1]
Ricardo Scotton[1]
Adilson Yoshio Furuse[1]
Carla Castiglia Gonzaga[1]

Corresponding author:
João César Zielak
Universidade Positivo
Rua Professor Pedro Viriato Parigot de Souza, n. 5.300 – Campo Comprido
CEP 81280-330 – Curitiba – PR – Brasil
E-mail: jzielak2@gmail.com

[1] Master's Program in Clinical Dentistry, Positivo University – Curitiba – PR – Brazil.
[2] Master's Program in Dentistry, Federal University of Paraná – Curitiba – PR – Brazil.

Received for publication: July 12, 2013. Accepted for publication: August 6, 2013.

Keywords:
biomechanics; dental implants; dental stress analysis; laboratory research.

Abstract

Objective: To demonstrate a colorimetric photoelastic analysis of tension distribution around dental implants under axial loads. **Material and methods:** Eight different designs of implant from two manufacturers were connected to their abutments, placed into epoxy resin blocks and observed under a polariscope coupled to a universal testing machine while subjected to axial loads of 5 N. The obtained images were quantitatively analyzed by image analysis software. **Results:** A strong correlation was found between the surface area and the implant fringe transition area (magenta color) of most samples (r = 0.908), and a moderate correlation was found between the fringe transition area and the mean thread height of the implants (r = 0.706, or r = 0.768 using a quadratic function). **Conclusion:** By this biomechanical study, it was possible to demonstrate a correlation of some implant characteristics to the colored fringe areas of tension distribution, a colorimetric method that can be used in comparative studies of photoelastic analysis. **Clinical significance:** An accurate planning and knowledge of oral implant biomechanics is important so that a safe and long-lasting

treatment can be achieved. This biomechanical study presented some correlations of the implant features and its photoelastic behavior, information that could be used by the practitioner while choosing the implant design for each clinical situation.

Introduction

The use of implants in the clinical practice of dentistry is becoming increasingly popular. Oral rehabilitation is founded on bone and gingival structures, and aims to restore both function and esthetics. Therefore, it is necessary for dental professionals to have a basic knowledge of biomechanics and engineering applicable to dentistry, including the distribution of tension within the tissues, to achieve a safe and long-lasting treatment. The selection of implants and their components, such as their design, length, and diameter, for a specific portion of the dental arch can exert a strong influence on the outcome of the implant [15].

Upon its introduction to clinical practice, oral rehabilitation with dental implants was considered to be very innovative, especially for the restoration of functional and esthetic characteristics in edentulous patients [3]. However, although a modern modality of oral rehabilitation has been established and its clinical effectiveness has been proved, several mechanical complications and limitations associated with dental implants still exist. Biological issues that involve the whole body demand special attention, such as tobacco usage, alcoholism, metabolic conditions, neurological disturbances, common systemic factors [29], and local (in situ) factors that can interfere with the quality and volume of bone and gingiva [21, 32, 38].

More recently, oral implantology has faced the new challenges of single and partial rehabilitations, which have made the development of alternative approaches necessary, especially regarding the esthetic requirements of the patient [20]. Thus, the integration of esthetic aspects with biomechanical function and a sense of balance among the tissues, prosthesis, and implant are essential for the achievement of clinical success.

Dental implants vary in their design and type of connection to the prosthesis. Abutments are the components responsible for the support of the artificial tooth crown [2], and can be classified as incorporating an external connection (EC, e.g. hexagon) or an internal connection (IC, e.g. hexagon, octagon, Morse cone and/or frictional, hybrid). With the exception of the implant with a frictional IC, all other implants have structured threads in order to fix the abutment to the implant body.

It is well recognized that bone resorption normally appears after prosthesis installation at the level of the first cervical threads of the implant; this depends not only on biological factors but also on mechanical factors [16]. However, clinical studies have demonstrated that this bone loss can be partially avoided by what is known as the switching platform method. In conventional systems, implants are rehabilitated with abutments of the same diameter as the connection platform. On the other hand, when using the switching platform method the abutments have smaller diameters, with the aim of increasing biological width [1] and preserving support tissue [8].

Many studies are conducted to obtain experimental data by simulating clinical situations, in order to evaluate the distribution of mechanical stress (tension) around implants and to study favorable or non-favorable characteristics of a certain implant design. To do so, methods that consider mathematical equations [2], finite element analysis [11, 28, 37], the use of frequency or resonance analysis [25], tomography images, microtomography, and photoelastic analysis [35] can be used, in isolation or in combination.

Photoelastic analysis is an experimental method used to determine the field of tensions and deformations in engineered parts or structures. It is a well-used method, especially in complex models [24], and can evaluate dimensional or tridimensional models. The method uses a polariscope, a simple optical device which consists of two polarized filters and a light source. Under a polariscope, photoelastic material produces colored fringes when normal light is used or black and white fringes when a monochromatic light is used. The fringes are associated with the tensions in the model studied [4, 7].

In the photoelastic studies, data have been reported by means of descriptive or complex calculations [9, 19, 23, 34]. Thus the aim of the present study was to demonstrate a colorimetric photoelastic analysis of tension distribution around dental implants under axial loads.

Material and methods

Eight different designs of implants were selected from two manufacturers (DSP, Dental Special Products, Campo Largo, PR, Brazil and Kopp Sistema de Implantes, Curitiba, PR, Brazil). The selected implants were representative of conventional systems (external hexagon implant-connection on cylindrical-conical or conical body with triangular threads) and switching platform systems (threaded Morse cone and frictional implant-abutment connection on cylindrical-conical or conical body with trapezoidal threads) (table I).

Table I – Selected implants and abutments

Group	Implant design	Implant dimension (mm)	Abutment dimension (mm)	Manufacturer
EC	Cy-co-Tra	3.75 x 11	4.1 x 10	B
	Cy-co-Tri	3.8 x 11.5	4.1 x 10	A
	Cy-co-Tra	5.0 x 11	4.1 x 10	B
	Co-Tri	5.0 x 11.5	5 x 10	A
IC	Co-Tra	3.75 x 11	4.5 x 13*	B
	Co-Tra	3.8 x 11.5	4.8 x 1.5 x 10	A
	Co-Tra	5.0 x 11	5.5 x 13*	B
	Cy-co-Tra	5.0 x 11.5	4.8 x 1.5 x 10	A

EC = external connection. IC = internal connection; Cy-co-Tra = cylindrical-conical body, trapezoidal threads; Cy-co-Tri = cylindrical-conical body, triangular threads; Co-Tri = conical body, triangular threads; Co-Tra = conical body, trapezoidal threads

* Frictional only

A = DSP, Dental Special Products, Campo Largo, PR, Brazil; B = Kopp Sistema de Implantes, Curitiba, PR, Brazil

All of the implants were connected to their abutments and placed into casts (40 mm height, 60 mm width, 10 mm depth), later filled with flexible epoxy resin (Flexivel GIII, Polipox, Sao Paulo, SP, Brazil) – this way no residual stresses were left in the samples – followed by the evaluation under a polariscope (Optovac, Osasco, SP, Brazil) coupled to a universal testing machine (DL30000, Emic, Sao Jose dos Pinhais, PR, Brazil). A 5 N axial load was applied. After 10 seconds of load application, photographs were taken (D5000, Nikon, Tokyo, Japan; 105 mm DG Macro EX, Sigma, Ronkonkoma, NY, USA).

In the obtained images, tension fringe transition areas (color between red and blue) were selected using Photoshop CS5 (Adobe Systems Incorporated, San Jose, CA, USA). The transition areas (TTA, total transition area) and their distance from the implant surface were measured (MDS, Maximum Distance from the transition area to the implant surface), and the characteristics of the implant such as surface area (SA), mean thread height (MTH), and mean thread distance (MTD) were evaluated with Image Tool 3.0 software (UTSCH, TX, USA). Data were then subjected to correlation analysis (SigmaPlot, Systat Software Inc., San Jose, CA, USA).

Results

From the image analysis (figures 1 and 2), it was possible to observe and measure the tension distribution patterns in every implant region (table II). The measured areas were localized at the medium and apical thirds of the implants. It was also possible to correlate the implants morphological features to the tension characteristics (table III). A strong correlation was found between the surface area of the implants and the fringe transition area of most samples ($n = 6$, $r = 0.908$) (figure 3). A moderate correlation was found between the fringe transition area and the mean thread height of each implant ($n = 6$, $r = 0.706$; $n = 8$, $r = 0.768$, using a quadratic function) (figures 4 and 5).

Table II – Values of fringe transition areas (mm^2) per implant region

Implant design	Cy-co-Tra	Cy-Co-Tri	Co-Tra	Co-Tra	Cy-co-Tra	Co-Tri	Co-Tra	Cy-co-Tra
Dimension	3.75 x 11	3.8 x 11.5	3.75 x 11	3.8 x 11.5	5 x 11	5 x 11.5	5 x 11	5 x 11.5
Region								
Cervical third	0.04	0	0	0	0	0	0	0.11
Medium third	0	0	0	0.09	0.09	0.17	0	0.23
Medium and apical thirds	0.14	0	0.17	2.3	7.77	2.39	0.45	3.96
Apical third	0.28	1.82	0.34	0.03	0.05	0.07	0.19	0.02
Apical vertex	0.14	0	0.26	0	0	0.02	1.15	0
Apex	0.04	0.1	0	0	0	0	0	0
Total	0.64	1.92	0.77	2.42	7.91	2.65	1.79	4.32

Cy-co-Tra = cylindrical-conical body, trapezoidal threads; Cy-co-Tri = cylindrical-conical body, triangular threads; Co-Tri = conical body, triangular threads; Co-Tra = conical body, trapezoidal threads

Table III – Measuring and obtained values

Ide	**Independent variables**				**Dependent variables**			
	IDi (mm)	**SA (mm^2)**	**MTH (mm)**	**MTD (mm)**	**TTA (mm^2)**	**MDS (mm)**		**NTA**
						Lateral	**Apical**	
Cy-co-Tra	3.75 x 11	54.07	0.37	0.5	0.64	0.4	1.85	2
Co-Tra	3.75 x 11	55.00	0.44	0.43	0.77	0.4	1.67	2
Cy-co-Tri	3.8 x 11.5	65.64	0.41	0*	1.92	1.11	0.37	2
Co-Tra	3.8 x 11.5	87.95	0.39	0.41	2.42	1.48	0	2
Co-Tri	5.0 x 11.5	95.06	0.41	0.41	4.32	3.78	0.14	2
Cy-co-Tra	5.0 x 11	105.95	0.32	0.44	7.91	4.94	0	2
Co-Tra	5.0 x 11	116.04	0.55	0.57	1.79	0.61	3.37	2
Co-Tri	5.0 x 11.5	117.41	0.57	0*	2.65	1.72	0	2

IDe = implant design; IDi = implant dimension; SA = surface area; MTH = mean thread height; MTD = mean between-thread distance; TTA = total tension transition area; MDS = maximum distance from the transition area to the implant surface, lateral and apical; NTA = number of transition areas analyzed per implant; Cy-co-Tra = cylindrical-conical body, trapezoidal threads; Cy-co-Tri = cylindrical-conical body, triangular threads; Co-Tri = conical body, triangular threads; Co-Tra = conical body, trapezoidal threads

* Depths of adjacent threads coincide

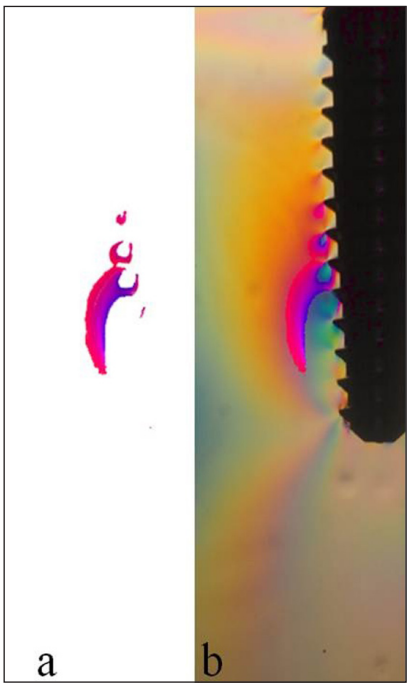

Figure 1 – Threaded Morse cone implant-abutment connection on conical body implant with trapezoidal threads (3.8 × 11.5 mm) loaded with 5 N. **(a)** Software-selected areas of fringe transition. **(b)** Polarized image of implant with software-selected areas (magenta)

Figure 2 – External hexagon implant-abutment connection on cylindrical-conical body with triangular threads (3.8 x 11.5 mm) loaded with 5 N. **(a)** Software-selected areas of fringe transition. **(b)** Polarized image of implant with software-selected areas (magenta)

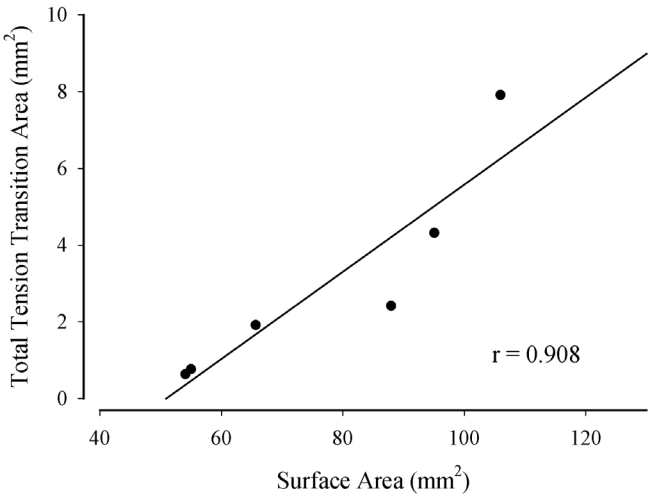

Figure 3 – Correlation of surface area with total tension transition area.

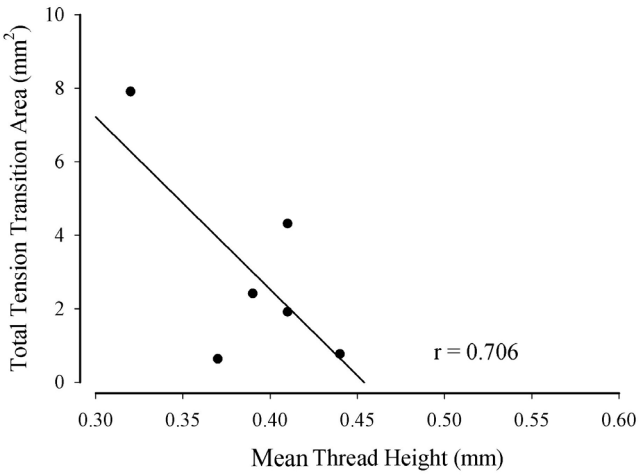

Figure 4 – Correlation of mean thread height with total tension transition area

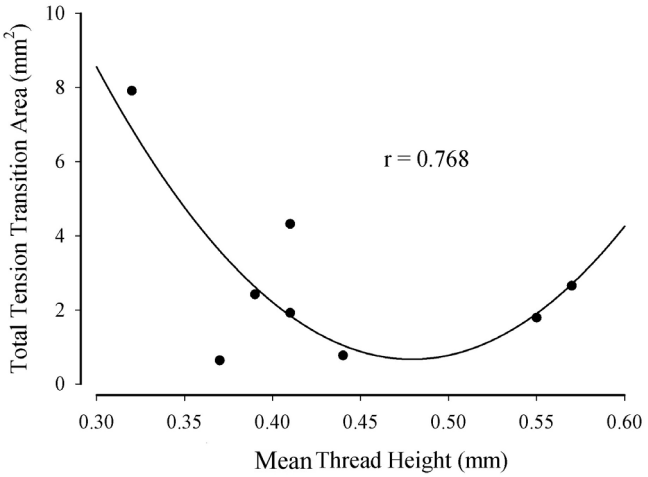

Figure 5 – Correlation of mean thread height with total tension transition area using a quadratic function

Discussion

In dentistry, there is a long-standing interest in the study of tension distribution, which includes the photoelastic research. Most of the literature concerns information regarding the relationship between implant body design and its potential to produce tensions around the implant [17, 18, 31, 33, 39]. According to Pesqueira *et al.* [27], one of the advantages of the photoelastic research is the possibility to observe tridimensional structures, such as oral implants, and the tension patterns all around their bodies, allowing the evaluation of the stress quality and magnitude. In studies of different implant designs, it is possible to find variations in tension distribution [10]; this was also demonstrated in the current study (table III).

The load value used in this study was 5 N, and although this value may seem low from the clinical perspective, in which mastication can reach values as high as 1000 N [12], it is necessary to consider that the applied load must be leveled to the physical properties of the supporting material (i.e. type of photoelastic resin). The flexible epoxy resin used in this study has much higher elasticity and lower resilience than human bone. In the present study, a small load was enough to cause a perceptible deformation under the polariscope. Clinically, this could probably simulate an implant being immediately loaded while into a cancellous bone, or perhaps in an over-instrumented surgical bone defect. Although apparently incompatible, elasticity and resilience are characteristics that achieve harmony within the mixture of organic and mineral content of bone tissue [6].

All of the implants tested presented tension concentration around the medium and apical third regions. Although this finding may be considered as positive, this information cannot be evaluated alone or extrapolated to the osseointegration mechanisms, since it is known that other factors including the chemistry and micromorphology of the implant surface may also influence the clinical success of the implant [22].

The data shown in table II reinforces this idea, as it was demonstrated that the regions with the largest areas of fringe transitions were located at the medium and apical thirds. Also, these large areas of fringe transitions were seen around the implants with the largest dimensions (5 × 11 mm = 7.91 mm^2; 5 × 11.5 mm = 4.32 mm^2). Conversely, the implants with the smallest dimensions produced the smallest total areas of fringe transitions (3.75 × 11 mm = 0.64 mm^2; 3.75 × 11 mm = 0.77 mm^2) – considering the fact that with the increase of the transition area the tension propagation decreases, and consequently diminishes the tension concentration. Thus, the implants with larger dimensions presented a tension distribution with lower potential for stress concentration, similarly to what has been previously demonstrated [26]. This result also agrees with the observations of Franz [13], who noted that low fringe propagation in turn leads to a low tension concentration. The importance of these transition areas also relates to the fact that the proximity of the fringes may represent a higher concentration of stress [14], indicating that where larger intervals between fringes exist there may be a dissociation of stress [37].

The figures 3, 4 and 5 demonstrated the correlation of data found in Table III. Although there is the need of an increase in the number of specimens for more reliable results, a few things can be pointed while evaluating these results. Implants with similar dimension and surface areas, such as the 3.75 x 11 mm (SA = 54.07 and 55.00 mm^2) produced total transition areas with a 20% discrepancy. The implants with the highest surface areas (5.0 x 11 or 11.5 mm, SA = 1.79 and 2.65 mm^2) were cut off from the correlation analysis, being totally out of the previous implant results pattern. As shown in figures 4 and 5 a previously published report confirms the influence of thread design on stress, using finite element analysis [37], but it is possible that other features of the implant not herein analyzed may also influence on the tension distribution around them – it is suggested that crown anatomical characteristics are also implicated into this matter [36]. Thus, in the present study, differences in the abutment design and type of connection may also have influenced these results – once it is known that the area of contact between the implant platform and the abutment may directly reflect the mechanical response to loads [5].

Despite its limitations, the photoelastic analysis allows for the observation of real structures [30], and it is important to emphasize that this original methodology may be a tool for a quantitative analysis that could be easily and statistically applied to any biomechanical study. Relevant photoelastic studies such as the one performed by Da Silva [9], for example, could also be quantitatively analyzed.

Therefore, for a more detailed investigation into the behavior patterns of dental implants using this reported photoelastic analysis, and for the achievement of more powerful results, current studies are being done with different load parameters and a higher number of specimens.

This study demonstrated a comparison of some dental implant characteristics to the photoelastic fringe areas of tension distribution, a simple method that can be applied to the vast area of biomechanics.

Conclusion

By this biomechanical study, it was possible to demonstrate a correlation of some implant characteristics to the colored fringe areas of tension distribution, a colorimetric method that can be used in comparative studies of photoelastic analysis.

Clinical significance

An accurate planning and knowledge of oral implant biomechanics is important so that a safe and long-lasting treatment can be achieved. This biomechanical study presented some correlations of the implant features and its photoelastic behavior, information that could be used by the practitioner while choosing the implant design for each clinical situation.

References

1. Berglundh TLJ. Dimension of the peri-implant mucosa. Biological width revisited. J Clin Periodontol. 1996;23:971-3.

2. Bozkaya D, Muftu S. Mechanics of the taper integrated screwed-in (TIS) abutments used in dental implants. J Biomech. 2005;38:87-97.

3. Brånemark PI, Hansson BO, Adell R, Breine U, Lindström J, Hallén O. Osseointegrated implants in the treatment of the edentulous jaw. Experience from a 10-year period. Scand J Plast Reconstr Surg Hand Surg. 1977;11:1-132.

4. Chang SH, Wu HH. Improvement of digital photoelasticity based on camera response function. Appl Opt. 2011;50:5263-70.

5. Chun HJ, Shin HS, Han CH, Lee SH. Influence of implant abutment type on stress distribution in bone under various loading conditions using finite element analysis. Int J Oral Maxillofac Implants. 2006;21:195-202.

6. Currey J. Incompatible mechanical properties in compact bone. J Theor Biol. 2004;231:569-80.

7. Dally JW, Riley WF (eds). Experimental stress analysis. Boston: McGraw-Hill College; 1991.

8. Danza M, Riccardo G, Carinci F. Bone platform switching: a retrospective study on the slope of reverse conical neck. Quintessence Int. 2010;41:35-40.

9. Da Silva EF, Pellizzer EP, Quinelli Mazaro JV, Garcia Junior IR. Influence of the connector and implant design on the implant-tooth-connected prostheses. Clin Implant Dent Relat Res. 2010;12:254-62.

10. Eser A, Tonuk E, Akca K, Cehreli MC. Predicting time-dependent remodeling of bone around immediately loaded dental implants with different designs. Med Eng Phys. 2010;32:22-31.

11. Fazel A, Aalai S, Rismanchian M, Sadr-Eshkevari P. Micromotion and stress distribution of immediate loaded implants: a finite element analysis. Clin Implant Dent Relat Res. 2009;11:267-71.

12. Ferrario VF, Sforza C, Zanotti G, Tartaglia GM. Maximal bite forces in healthy young adults as predicted by surface electromyography. J Dent. 2004;32:451-7.

13. Franz T. Photoelastic study of the mechanic behavior of orthotropic composite plates subjected to impact. Comp Struct. 2001;54:169-78.

14. French AA, Bowles CQ, Parham PL, Eick JD, Killoy WJ, Cobb CM. Comparison of peri-implant stresses transmitted by four commercially available osseointegrated implants. Int J Periodontics Restorative Dent. 1989;9:221-30.

15. Galanis CC, Sfantsikopoulos MM, Koidis PT, Kafantaris NM, Mpikos PG. Computer methods for automating preoperative dental implant planning: implant positioning and size assignment. Comput Methods Programs Biomed. 2007;86:30-8.

16. Hagiwara Y. Does platform switching really prevent crestal bone loss around implants? Jpn Dent Sci Rev. 2010;46:122-31.

17. Irvin AW, Webb EL, Holland GA, White JT. Photoelastic analysis of stress induced from insertion of self-threading retentive pins. J Prosthet Dent. 1985;53:311-6.

18. Junior SM, Asprino L, Moraes MD. Photoelastic analysis of stress distribution of surgically assisted rapid maxillary expansion with and without separation of the pterygomaxillary suture. J Oral Maxillofac Surg. 2011;69:1771-5.

19. Kim KS, Kim YL, Bae JM, Cho HW. Biomechanical comparison of axial and tilted implants for mandibular full-arch fixed prostheses. Int J Oral Maxillofac Implants. 2011;26:976-84.

20. Knoernschild KL. Early survival of single-tooth implants in the esthetic zone may be predictable despite timing of implant placement or loading. J Evid Based Dent Pract. 2010;10:52-5.

21. Kwasnicki A, Butterworth C. 360 degrees peri-implant, keratinised, soft-tissue grafting with stereolithographic-aided dressing plate. Int J Oral Maxillofac Surg. 2009;38:87-90.

22. Löberg J, Mattisson I, Hansson S, Ahlberg E. Characterisation of titanium dental implants I: critical assessment of surface roughness parameters. Open Biomat J. 2010;2:18-35.

23. Lopes JNI, Lucas BD, Gomide HA, Gomes VL. Impression techniques for multiple implants: a photoelastic analysis. Part I: comparison of three direct methods. J Oral Implantol. 2011.

24. Mahler DB, Peyton FA. Photoelasticity as a research technique for analyzing stresses in dental structures. J Dent Res. 1955;34:831-8.

25. Pattijn V, Van Lierde C, Van der Perre G, Naert I, Vander Sloten J. The resonance frequencies and mode shapes of dental implants: Rigid body behaviour versus bending behaviour. A numerical approach. J Biomech. 2006;39:939-47.

26. Pellizzer EP, Falcon-Antenucci RM, de Carvalho PS, Santiago JF, de Moraes SL, de Carvalho BM. Photoelastic analysis of the influence of platform switching on stress distribution in implants. J Oral Implantol. 2010;36:419-24.

27. Pesqueira A, Goiato M, Gennari-Filho H, Monteiro D, Dos Santos D, Haddad M et al. The use of stress analysis methods to evaluate the biomechanics of oral rehabilitation with implants. J Oral Implantol. 2012 [Epub ahead of print].

28. Pessoa RS, Muraru L, Junior EM, Vaz LG, Sloten JV, Duyck J et al. Influence of implant connection type on the biomechanical environment of immediately placed implants - CT-based nonlinear, three-dimensional finite element analysis. Clin Implant Dent Relat Res. 2010;12:219-34.

29. Pye AD, Lockhart DE, Dawson MP, Murray CA, Smith AJ. A review of dental implants and infection. J Hosp Infect. 2009;72:104-10.

30. Rossi F, Zavanelli AC, Zavanelli RA. Photoelastic comparison of single tooth implant-abutment bone of platform switching vs conventional implant designs. J Contemp Dent Pract. 2011;12:124-30.

31. Sauveur G, Boccara E, Colon P, Sobel M, Boucher Y. A photoelastimetric analysis of stress induced by root-end resection. J Endod. 1998;24:740-3.

32. Shibli JA, Aguiar KC, Melo L, d'Avila S, Zenobio EG, Faveri M et al. Histological comparison between implants retrieved from patients with and without osteoporosis. Int J Oral Maxillofac Surg. 2008;37:321-7.

33. Suzuki M, Kamezawa H, Yokozuka S. 2-dimensional photoelastic stress analysis of the alveolar bone with an S-type Bioceram implant under a free-end bridge. Shigaku. 1985;73:831-44.

34. Tonella BP, Pellizzer EP, Ferraco R, Falcon-Antenucci RM, Carvalho PS, Goiato MC. Photoelastic analysis of cemented or screwed implant-supported prostheses with different prosthetic connections. J Oral Implantol. 2011;37:401-10.

35. Ueda C, Markarian RA, Sendyk CL, Lagana DC. Photoelastic analysis of stress distribution on parallel and angled implants after installation of fixed prostheses. Braz Oral Res. 2004;18:45-52.

36. Wang MQ, Zhang M, Zhang JH. Photoelastic study of the effects of occlusal surface morphology on tooth apical stress from vertical bite forces. J Contemp Dent Pract. 2004;5:74-93.

37. Winter W, Steinmann P, Holst S, Karl M. Effect of geometric parameters on finite element analysis of bone loading caused by nonpassively fitting implant-supported dental restorations. Quintessence Int. 2011;42:471-8.

38. Wood MR, Vermilyea SG. A review of selected dental literature on evidence-based treatment planning for dental implants: report of the Committee on Research in Fixed Prosthodontics of the Academy of Fixed Prosthodontics. J Prosthet Dent. 2004;92:447-62.

39. Ziada HM, Benington IC, Orr JF. Photoelastic stress analysis in resin bonded bridge design. Eur J Prosthodont Restor Dent. 1995;3:217-22.